RECENT CLEO RESULTS ON HADRON SPECTROSCOPY*

Tomasz Skwarnicki

Department of Physics, 201 Physics Building, Syracuse University
Syracuse, NY 13244, USA

(Received May 18, 2005)

Selected CLEO results on hadron spectroscopy are reviewed.

PACS numbers: 14.40.Gx, 13.20.Gd, 13.25.Ft

1. Introduction

The CLEO experiment at CESR has been in operation for over a quarter of century. Most of its past running was performed at the $\Upsilon(4S)$ for B meson physics, with smaller amount of data taken at the narrow $\Upsilon(1S, 2S, 3S)$ resonances and at the $\Upsilon(5S)$. With advent of two-ring B-factories at KEK and SLAC, single-ring CESR could not keep up with luminosity. CESR instantaneous peak luminosity at the $\Upsilon(4S)$ is 1.2×10^{33} cm^{-2}s^{-1} compared to a KEK-B (PEP-II) record of $1.5\,(0.9) \times 10^{34}$ cm^{-2}s^{-1}. Therefore, the B-physics runs ended in mid 2001. Longer runs at the narrow Υ resonances followed, increasing the data sizes available for these resonances by an order of magnitude; 29×10^6, 9×10^6 and 6×10^6 resonant decays were recorded for $\Upsilon(1S)$, $\Upsilon(2S)$ and $\Upsilon(3S)$, respectively. Some data were also taken at the $\Upsilon(5S)$ (and above) for exploration of B_s (Λ_b) production rates.

Then, CESR was reconfigured by insertion of additional wiggler magnets to operate at lower beam energies in the charm threshold region. Initial test runs with one new wiggler, performed in fall 2002, provided useful $\psi(2S)$ data. More data were taken in fall 2003 with six wigglers and a new vertex detector installed in CLEO (the radiation damaged silicon detector was replaced by a MWPC with all stereo wires). Since fall 2004 the CESR-c has been operating with 12 wiggler magnets. Instantaneous luminosity reached so far, 6.4×10^{31} cm^{-2}s^{-1}, is lower than previous optimistic projections of

* Presented at the Cracow Epiphany Conference on Hadron Spectroscopy, Cracow, Poland, January 6–8, 2005.

3×10^{32} cm^{-2}s^{-1}, but still orders of magnitude higher than achieved by BEPC, 5×10^{30} cm^{-2}s^{-1}, or SPEAR-II, 6×10^{29} cm^{-2}s^{-1}. Eventually, the BEPC-II two-ring machine, under constructions in China, will deliver luminosity of an order of 1×10^{33} cm^{-2}s^{-1} at these energies.

The data collected so far by CLEO at the charm threshold consist of 6 pb^{-1} (3.1×10^6 resonant decays) at the $\psi(2S)$, 20 pb^{-1} at the continuum below $\psi(2S)$ and 280 pb^{-1} at $\psi(3770)$. Even though the BES experiment collected 4.5 more $\psi(2S)$ decays, our $\psi(2S)$ sample has unique features since CLEO is the first detector studying the charmonium system with excellent detection of both: charged particles [1] (including particle identification [2]) and photons [3]. The $\psi(3770)$ sample, used to study D meson decays, is a factor of 10 larger than previously collected for the $D^0\bar{D}^0$, D^+D^- pairs produced nearly at rest.

The results discussed is this article include results for hadronic parameters of the D mesons and various studies on long-lived charmonium and bottomonium states.

2. Measurement of f_D

Measurement of the decay constant, f_D, is important for cross-checks of theoretical calculations of this quantity, lattice QCD calculations in particular. Similar calculations are employed for hadronic quantities of B mesons and used for extraction of the CKM parameters. We measure this decay constant by determining $\mathcal{B}(D^- \to \mu^-\bar{\nu}_\mu)$. The muon is detected to-

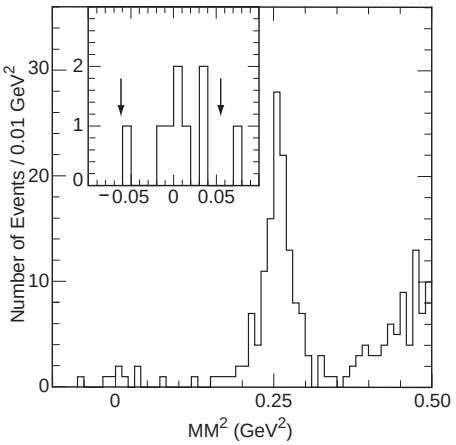

Fig. 1. MM^2 distribution for selected events. The large peak around 0.25 GeV^2 is from $D^+ \to K^0_{\rm L}\pi^+$. The inset shows the signal region for $D^+ \to \mu^+\nu_\mu$ enlarged; the $\pm 2\sigma$ range is shown between the two arrows.

gether with all decay products of the other charged D in the event. The following decay modes are used on the tag side: $K^-\pi^+\pi^+$, $K^-\pi^+\pi^+\pi^0$, $K^0_S\pi^+\pi^0$, $K^0_S\pi^+$, $K^0_S\pi^+\pi^-\pi^+$. Then the missing-mass squared is calculated, $\mathrm{MM}^2 = (E_{\mathrm{beam}} - E_\mu)^2 - (-\vec{P}_{D_{\mathrm{tag}}} - \vec{P}_\mu)^2$. The signal events are expected to peak at $\mathrm{MM}^2 = m^2_\nu = 0$. Using 60 pb^{-1} of the 6 wiggler data collected at $\psi(3770)$ (2.9×10^4 tagged D events), 8 events are observed in the signal region, whereas 1 background event is expected (see Fig. 1). This is the first statistically compelling evidence for $D^- \to \mu^-\bar{\nu}_\mu$ decay. From the measured branching ratio, $(3.5 \pm 1.4 \pm 0.6) \times 10^{-4}$, we determine, $f_{D^-} = (202 \pm 41 \pm 17)$ MeV. More detailed description of this analysis can be found elsewhere [4]. At present, the experimental errors are too large to provide sensitive tests of the theoretical calculations. More data are being analyzed.

3. Branching ratios for hadronic decays of D mesons

Precise measurements of hadronic D decays are of great importance since, for example, they are often used to normalize B and D semileptonic branching ratios, which in turn are used to extract CKM matrix elements. We determine hadronic branching ratios for D mesons at the $\psi(3770)$ resonance using double-tag method. The analysis is described in detail elsewhere [5]. The results, based on the partial data set of about 60 pb^{-1}, are given in Table I, where they are also compared to the world average values. We have already reached sensitivity comparable to the errors on the world average values. Our future goal is to reduce the relative errors to 1–2 % for the major decay modes.

TABLE I

Branching fractions measured by CLEO compared to the world average values.

Parameter	CLEO-c	PDG 2004
$\mathcal{B}(D^0 \to K^-\pi^+)$	$(3.91 \pm 0.08 \pm 0.09)\%$	$(3.80 \pm 0.09)\%$
$\mathcal{B}(D^0 \to K^-\pi^+\pi^0)$	$(14.9 \pm 0.3 \pm 0.5)\%$	$(13.0 \pm 0.8)\%$
$\mathcal{B}(D^0 \to K^-\pi^+\pi^+\pi^-)$	$(8.3 \pm 0.2 \pm 0.3)\%$	$(7.5 \pm 0.3)\%$
$\mathcal{B}(D^+ \to K^-\pi^+\pi^+)$	$(9.5 \pm 0.2 \pm 0.3)\%$	$(9.2 \pm 0.6)\%$
$\mathcal{B}(D^+ \to K^-\pi^+\pi^+\pi^0)$	$(6.0 \pm 0.2 \pm 0.2)\%$	$(6.5 \pm 1.1)\%$
$\mathcal{B}(D^+ \to K^0_S\pi^+)$	$(1.55 \pm 0.05 \pm 0.06)\%$	$(1.41 \pm 0.09)\%$
$\mathcal{B}(D^+ \to K^0_S\pi^+\pi^0)$	$(7.2 \pm 0.2 \pm 0.4)\%$	$(4.9 \pm 1.5)\%$
$\mathcal{B}(D^+ \to K^0_S\pi^+\pi^+\pi^-)$	$(3.2 \pm 0.1 \pm 0.2)\%$	$(3.6 \pm 0.5)\%$
$\mathcal{B}(D^+ \to K^+K^-\pi^+)$	$(0.97 \pm 0.04 \pm 0.04)\%$	$(0.89 \pm 0.08)\%$

4. Observation of $h_c(1^1P_1)$ state

Spin–spin forces in heavy quarkonia are predicted to be short-range. Thus, while significant hyperfine splitting is observed for charmonium S-states (*e.g.* 116 MeV for $n = 1$), the mass splitting between the singlet state ($h_c(1^1P_1)$) and the center-of-gravity of the spin-triplet states

$$\frac{\sum_J (2J+1)\, m(\chi_c(1^3P_J))}{\sum_J (2J+1)}$$

is expected to be small. The $h_c(1^1P_1)$ was sighted previously twice in $\bar{p}p$ annihilation at two different masses [6] with marginal statistical significance. Higher statistics searches disproved these observations. We present highly significant evidence for this state, settling the question about its mass.

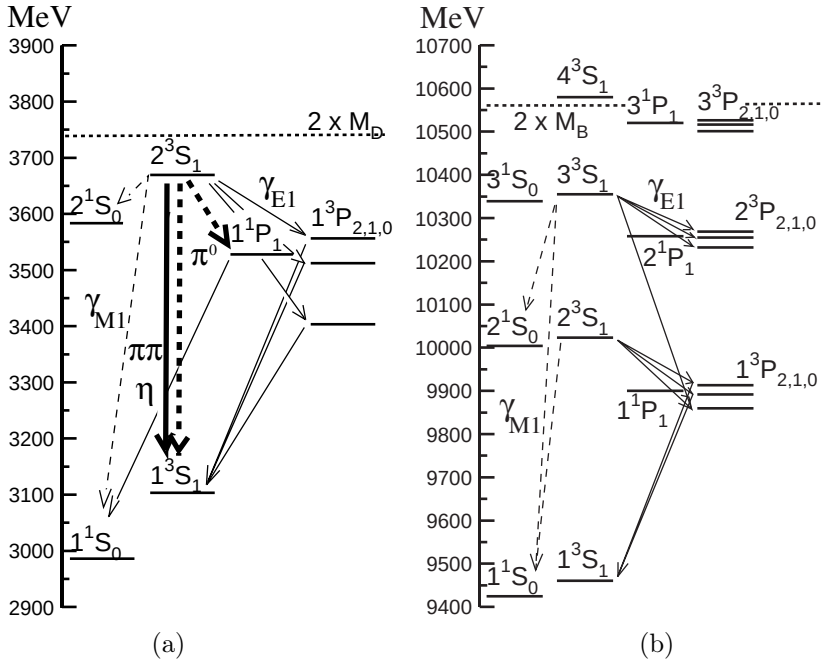

Fig. 2. Various transitions in: (a) $c\bar{c}$, and (b) $b\bar{b}$ systems discussed in this article. The E1 (M1) photon transitions are indicated by the thin solid (dashed) lines. The $\pi\pi$,η (π^0) transitions are indicated by the thick solid (dashed) lines.

We have observed the $h_c(1P)$ state in isospin violating π^0 transitions from the $\psi(2S)$ resonance, followed by a highly favored E1 photon transition, $h_c(1P) \to \gamma\eta_c(1S)$ (see Fig. 2(a)). Two essentially statistically independent approaches are used. In the inclusive approach, the $\eta_c(1S)$ is allowed to decay to anything. This approach results in a higher signal efficiency but

also higher backgrounds. After imposing consistency of the reconstructed $\pi^0(\rightarrow \gamma\gamma)\gamma$ pair with the $\psi(2S)$ to $\eta_c(1S)$ transition, the π^0-recoil mass is plotted (Fig. 3(a)). The photon four-vectors in the π^0 decay are constrained to the π^0 mass, substantially improving the recoil mass resolution. A peak of 150 ± 40 events, with a significance of 3.8 standard deviations, is observed.

In the second, exclusive, approach the $\eta_c(1S)$ is reconstructed in one of the following decay modes: $K^0_S K^{\pm}\pi^{\mp}$, $K^0_L K^{\pm}\pi^{\mp}$, $K^+K^-\pi^+\pi^-$, $\pi^+\pi^-\pi^+\pi^-$, $K^+K^-\pi^0$, $K^+K^-\eta(\rightarrow \gamma\gamma$ or $\rightarrow \pi^+\pi^-\pi^0)$. Particle ID capabilities of the CLEO detector (RICH [2] and dE/dX) are critical in this analysis. The $\eta_c(1S)$ reconstruction was optimized on the hindered M1 photon transitions: $\psi(2S) \rightarrow \gamma\eta_c(1S)$ (see Fig. 2(a)). This approach results in excellent background suppression, but also in smaller signal efficiency. The π^0-recoil mass for the exclusive analysis is plotted in Fig. 3(b). A peak of 17.5 ± 4.5 events is observed at the mass consistent with the inclusive analysis. The probability of the background fluctuating up to produce this peak is equivalent to a signal significance of 6.1 standard deviations.

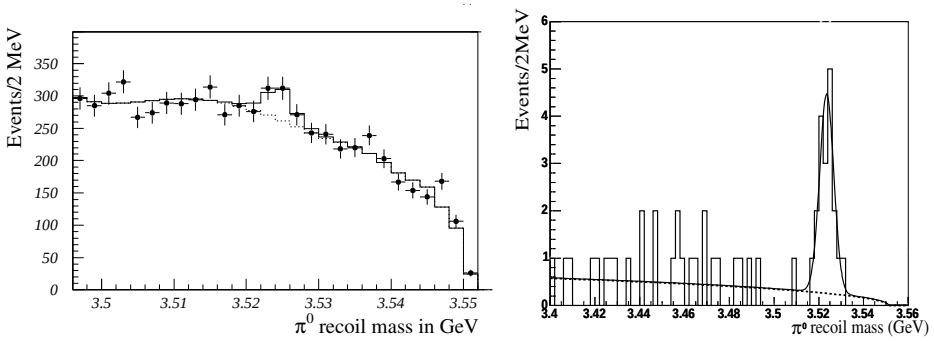

(a) (b)

Fig. 3. Recoil mass against the reconstructed π^0 in: (a) inclusive, and (b) exclusive search for the h_c state. The fits are superimposed on the data.

The average of the inclusive and exclusive mass measurements, $3524.4 \pm 0.6 \pm 0.4$ MeV, is $1.0 \pm 0.6 \pm 0.4$ MeV below the center-of-gravity of the $\chi_{cJ}(1P)$ states, confirming the conventional picture of spin-spin interactions. The measured product branching ratio, $\mathcal{B}(\psi(2S) \rightarrow \pi^0 h_c(1P)) \times \mathcal{B}(h_c(1P) \rightarrow \gamma\eta_c(1S)) = (4.0 \pm 0.8 \pm 0.7) \times 10^{-4}$, is in the midrange of the theoretical predictions [7], which vary by 2 orders of magnitude due to difficulties in predicting the π^0 transition width.

5. Survey of $\psi(2S)$ to $J/\psi(1S)$ transitions

We have performed a survey of $\psi(2S)$ to $J/\psi(1S)$ transitions, tagging J/ψ by its annihilation to electron or muon pairs (l^+l^-). The $\mathcal{B}(\psi(2S) \to XJ/\psi(1S))$ is measured from the J/ψ peak observed in the inclusive dilepton mass distribution. Transition branching ratios for individual channels are measured by full reconstruction of the following exclusive event samples: $\pi^+\pi^-l^+l^-$, $\pi^0\pi^0l^+l^-$, $\eta(\to \gamma\gamma$ or $\to \pi^+\pi^-\pi^0)l^+l^-$, $\pi^0(\to \gamma\gamma)l^+l^-$, $\gamma\chi_{cJ} \to \gamma\gamma l^+l^-$ (see Fig. 2(a)). The backgrounds are small and dominated by feed-across between the transition modes. They are subtracted using Monte Carlo simulations. The large statistics, the small backgrounds and the large, well-understood detector acceptance result in the precision measurements. The results are compared to previous measurements in Table II. A more detailed description of this analysis can be found elsewhere [8]. These are the most

TABLE II

The CLEO results [8] for $\psi(2S)$ to $J/\psi(1S)$ transitions compared to the PDG fit values [9] and two recently published measurements by BES [10] and E835 [11].

Channel	$\mathcal{B}$ (%)		
	CLEO	PDG 2004	E835
$\pi^+\pi^- J/\psi$	$33.54 \pm 0.14 \pm 1.10$	31.7 ± 1.1	$29.2 \pm 0.5 \pm 1.8$
$\pi^0\pi^0 J/\psi$	$16.52 \pm 0.14 \pm 0.58$	18.8 ± 1.2	$16.7 \pm 0.5 \pm 1.4$
$\eta J/\psi$	$3.25 \pm 0.06 \pm 0.11$	3.16 ± 0.22	$2.8 \pm 0.2 \pm 0.2$
$\pi^0 J/\psi$	$0.13 \pm 0.01 \pm 0.01$	0.10 ± 0.02	
$\gamma\chi_{c0} \to \gamma\gamma J/\psi$	$0.18 \pm 0.01 \pm 0.02$	0.10 ± 0.01	
$\mathcal{B}(\chi_{c0} \to \gamma J/\psi)$	2.0 ± 0.3	1.2 ± 0.1	
$\gamma\chi_{c1} \to \gamma\gamma J/\psi$	$3.44 \pm 0.06 \pm 0.13$	2.67 ± 0.15	
$\mathcal{B}(\chi_{c1} \to \gamma J/\psi)$	37.9 ± 2.2	31.6 ± 3.3	
$\gamma\chi_{c2} \to \gamma\gamma J/\psi$	$1.85 \pm 0.04 \pm 0.07$	1.30 ± 0.08	
$\mathcal{B}(\chi_{c2} \to \gamma J/\psi)$	19.9 ± 1.3	20.2 ± 1.7	
XJ/ψ	$59.50 \pm 0.15 \pm 1.90$	57.6 ± 2.0	
	$\mathcal{B}/\mathcal{B}_{\pi^+\pi^- J/\psi}$ (%)		
	CLEO	BES	
$\pi^0\pi^0 J/\psi$	$49.24 \pm 0.47 \pm 0.86$	$57.0 \pm 0.9 \pm 0.3$	
$\eta J/\psi$	$9.68 \pm 0.19 \pm 0.13$	$9.8 \pm 0.5 \pm 1.0$	
$\gamma\chi_{c1} \to \gamma\gamma J/\psi$	$10.24 \pm 0.17 \pm 0.23$	$12.6 \pm 0.3 \pm 3.8$	
$\gamma\chi_{c2} \to \gamma\gamma J/\psi$	$5.52 \pm 0.13 \pm 0.13$	$6.0 \pm 0.1 \pm 2.8$	
XJ/ψ	$1.77 \pm 0.01 \pm 0.02$	$1.87 \pm 0.03 \pm 0.06$	

precise measurements to date. The difference between the inclusive and the sum over exclusive branching ratios is $(0.6 \pm 0.4)\%$, leaving little room for other, yet undetected modes. Unlike previous measurements, the $\pi^0\pi^0$ rate is half of the $\pi^+\pi^-$ rate, as expected from the isospin symmetry. The branching ratios for two-photon cascades via the $\chi_{c0,1}$ states are significantly higher than previously measured, which leads to significantly larger rates for $\chi_{c0,1} \to \gamma J/\psi$.

6. Measurement of $\mathcal{B}(\Upsilon(nS) \to \mu^+\mu^-)$

Measurement of dimuon decay rates of the narrow Υ resonances is important for determination of their total widths ($\Gamma_{\rm tot} = \Gamma_{ee}/\mathcal{B}(\Upsilon(nS) \to \mu^+\mu^-)$). It is accomplished by counting on- and off-resonance $\mu^+\mu^-$ and hadronic event yields. Since the continuum background subtraction is substantial, especially for the mu-pair yields, 20–30% of the data were accumulated below the resonance peaks. The analysis details can be found elsewhere [17]. The CLEO results are given in Table III, where they are also compared to the world average values. The precision of our determination is comparable or better than the errors on the world average values. While agreement for the $\Upsilon(1S)$ is excellent, we obtain significantly larger values for the $\Upsilon(2S)$ and $\Upsilon(3S)$ resonances. This, in turn leads to significantly smaller estimates of their total widths, which impacts many comparisons between the data and theory for transitions widths of these resonances (see *e.g.*, next section).

TABLE III

Dimuon branching ratios and total widths of the narrow Υ resonances.

Resonance	$\mathcal{B}(\Upsilon(nS) \to \mu^+\mu^-)$	
	CLEO	PDG 2004
$\Upsilon(1S)$	$(2.49 \pm 0.02 \pm 0.07)\%$	$(2.48 \pm 0.06)\%$
$\Upsilon(2S)$	$(2.03 \pm 0.03 \pm 0.08)\%$	$(1.31 \pm 0.21)\%$
$\Upsilon(3S)$	$(2.39 \pm 0.07 \pm 0.10)\%$	$(1.81 \pm 0.17)\%$
	$\Gamma_{\rm tot}(\Upsilon(nS))$	
	CLEO	PDG 2004
$\Upsilon(1S)$	(52.8 ± 1.8) keV	(53.0 ± 1.5) keV
$\Upsilon(2S)$	(29.0 ± 1.6) keV	(43.0 ± 6.0) keV
$\Upsilon(3S)$	(20.3 ± 2.1) keV	(26.3 ± 3.4) keV

7. Photon transitions in charmonium and bottomonium systems

We have analyzed inclusive photon spectra in the $\psi(2S)$, $\Upsilon(2S)$ and $\Upsilon(3S)$ data for monochromatic photons due to E1 and M1 photon transitions (see Fig. 2). The results have been published and can be found elsewhere [12].

From the measurements of photon energies in the dominant E1 transitions, $n^3S_1 \to \gamma(n-1)^3P_{2,1,0}$, ratios of the fine splittings in the triplet-P states, $r \equiv (M_2 - M_1)/(M_1 - M_0)$, are determined with a high precision: $0.490 \pm 0.002 \pm 0.003$ ($1P$ $c\bar{c}$), $0.57 \pm 0.01 \pm 0.01$ ($1P$ $b\bar{b}$) and $0.58 \pm 0.01 \pm 0.01$ ($2P$ $b\bar{b}$). Somewhat surprisingly, the latter two are essentially equal.

In the non-relativistic limit, the E1 matrix elements for these transitions are J independent. Thus, a ratio of the branching ratios ($\mathcal{B}(^3S_1 \to \gamma^3P_J)$) corrected for the phase-space factors ($(2J+1)E_\gamma^3$) is expected to be 1 for any combination of J values. The results are summarized in Table IV. While the $(J=2)/(J=1)$ ratios in the $b\bar{b}$ system reproduce this expectation, the rates to the $J=0$ state are lower. Relativistic corrections were predicted to be, in fact, the largest for the transitions to $^3P_0$ state [13]. The ratios in the $c\bar{c}$ system are far from the non-relativistic prediction, apparently affected by the lighter quark mass and the $2^3S_1 - 1^3D_1$ mixing.

TABLE IV

Ratio of $\mathcal{B}(n^3S_1 \to \gamma(n-1)^3P_J)/(2J+1)E_\gamma^3$ as measured by CLEO for various J combinations in the charmonium and bottomonium systems.

Final state	$(J=2)/(J=1)$	$(J=0)/(J=1)$	$(J=0)/(J=2)$
$\chi_b(2P)$	$1.00 \pm 0.01 \pm 0.05$	$0.76 \pm 0.02 \pm 0.07$	$0.76 \pm 0.02 \pm 0.09$
$\chi_b(1P)$	$1.01 \pm 0.02 \pm 0.08$	$0.82 \pm 0.02 \pm 0.06$	$0.81 \pm 0.02 \pm 0.11$
$\chi_c(1P)$	$1.50 \pm 0.02 \pm 0.05$	$0.86 \pm 0.01 \pm 0.06$	$0.59 \pm 0.01 \pm 0.05$

The absolute values of the branching ratios are also significantly below the non-relativistic predictions for the $c\bar{c}$ system. Relativistic corrections are needed to explain the observed rates, as illustrated in Fig. 4. In contrast, the relativistic corrections in the $b\bar{b}$ system are not large and even non-relativistic calculations give a reasonable description of the data. This is true only for the dominant E1 transitions. The E1 matrix elements for the $3^3S_1 \to \gamma 1^3P_J$ transitions are expected to be small, reflecting large cancellations in the integral of the dipole operator between the 3^3S_1 and 1^3P_J states. The relativistic corrections, and therefore the J dependence, are expected to be large. We have measured the $J=0$ rate for the first time. The theoretical predictions are scattered in a wide range and only a few models match our data well (see Fig. 5).

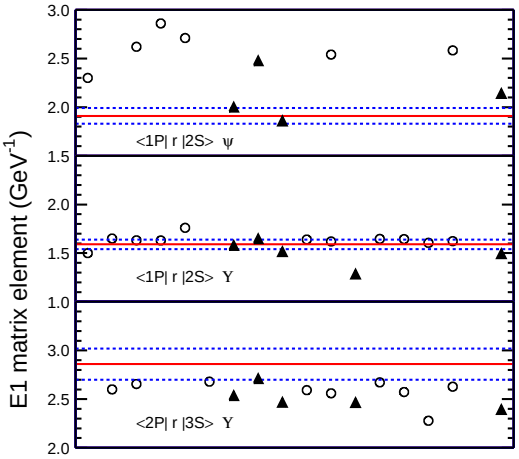

Fig. 4. Measured and predicted values of matrix elements for E1 transitions in heavy quarkonia. The rates are averaged over different spins of the triplet P states. The measured values are calculated from the CLEO branching ratio results (and total widths of the triplet S states [9, 17]). The central values and error bars for the measured values are indicated by the solid and dashed lines respectively. Circles (triangles) show non-relativistic (relativistic) calculations. The relativistic calculations are averaged over spins with the same weights as the data. The predictions [18] are ordered according to the publication date.

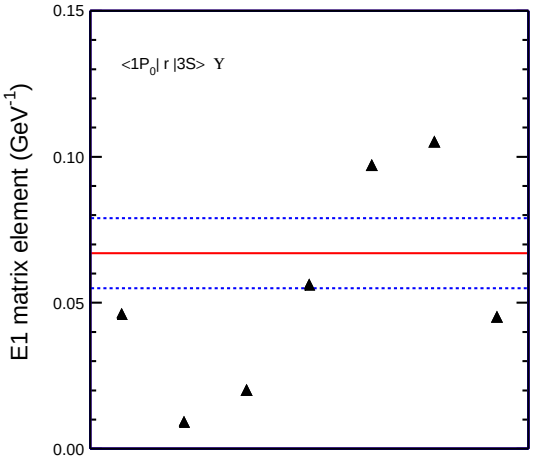

Fig. 5. Measured and predicted values of E1 matrix element for $\Upsilon(3S) \to \gamma\chi_b(1P_0)$. The measured value is calculated from the CLEO results for the branching ratio and the total width of the $\Upsilon(3S)$ [17]. The central values and error bars for the measured values are indicated by the solid and dashed lines, respectively. The predictions [19] (triangles) are ordered according to the publication date.

While we have confirmed the hindered M1 transition $\psi(2S) \to \gamma\eta_c(1S)$, previously observed by Crystal Ball [14], their signal for the direct M1 transition $\psi(2S) \to \gamma\eta_c(2S)$ [15] is not observed in our data. This is not surprising in view of the recent $\eta_c(2S)$ mass measurements [16], which are inconsistent with the $\eta_c(2S)$ mass claimed by Crystal Ball. Searches for hindered M1 transitions in the $b\bar{b}$ system resulted in upper limits only, thus no singlet $b\bar{b}$ state has been observed to date. Only the most recent theoretical estimates of the expected M1 rates are consistent with all $c\bar{c}$ and $b\bar{b}$ data, and only marginally so with our limit on $\mathcal{B}(\Upsilon(3S) \to \gamma\eta_b(1S))$ (see Fig. 6).

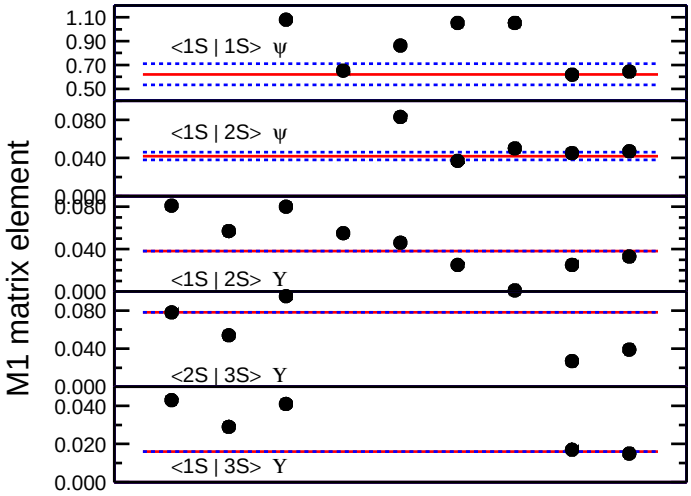

Fig. 6. Measured and predicted values of matrix elements for M1 transitions in heavy quarkonia. The measured values are calculated from the CLEO branching ratio results (and total widths of the triplet S states [9, 17]), except for the direct M1 transition, $2S \to 1S$, where the world average branching ratio [9] is used. The central values and error bars for the measured values are indicated by the solid and dashed lines, respectively. The solid lines for the M1 transitions in the Υ system show the experimental upper limits. The predictions [20] (points) are ordered according to the publication date.

I would like to thank the organizers of the conference for hospitality and support. I would also like to thank my CLEO colleagues for the input to this article. This work was supported by the National Science Foundation and the U.S. Department of Energy.

REFERENCES

[1] D. Peterson *et al.*, *Nucl. Instrum. Methods Phys. Res.* **A478**, 142 (2002); G. Viehhauser *et al.*, *Nucl. Instrum. Methods Phys. Res.* **A462**, 146 (2001).

[2] M. Artuso *et al.*, *Nucl. Instrum. Methods Phys. Res.* **A502**, 91 (2003).

[3] CLEO Collaboration, Y. Kubota *et al.*, *Nucl. Instrum. Methods Phys. Res.* **A320**, 66 (1992).

[4] CLEO Collaboration, G. Bonvicini *et al.*, *Phys. Rev.* **70**, 112004 (2004).

[5] CLEO Collaboration, Q. He *et al.*, `hep-ex/0504003`.

[6] R704 Collaboration, C. Baglin *et al.*, *Phys. Lett.* **B171**, 135 (1986); E760 Collaboration, T.A. Armstrong *et al.*, *Phys. Rev. Lett.* **69**, 2337 (1992).

[7] S. Godfrey, J.L. Rosner, *Phys. Rev.* **D66**, 014012 (2002); D. Joffe, Ph.D. thesis, Northwestern University, 2004.

[8] CLEO Collaboration, N.E. Adam *et al.*, `hep-ex/0503028`.

[9] Particle Data Group, S. Eidelman *et al.*, *Phys. Lett.* **B592**, 1 (2004).

[10] BES Collaboration, M. Ablikim *et al.*, *Phys. Rev.* **D70**, 012003 (2004).

[11] E835 Collaboration, M. Andreotti *et al.*, *Phys. Rev.* **D71**, 032006 (2005).

[12] CLEO Collaboration, M. Artuso *et al.*, *Phys. Rev. Lett.* **94**, 032001 (2005); S.B. Athar *et al.*, *Phys. Rev.* **D70**, 112002 (2004).

[13] P. Moxhay, J.L. Rosner, *Phys. Rev.* **D28**, 1132 (1983); R. McClary, N. Byers, *Phys. Rev.* **D28**, 1692 (1983).

[14] Crystal Ball Collaboration, J.E. Gaiser *et al.*, *Phys. Rev.* **D34**, 711 (1986).

[15] Crystal Ball Collaboration, C. Edwards *et al.*, *Phys. Rev. Lett.* **48**, 70 (1982).

[16] Belle Collaboration, S.K. Choi *et al.*, *Phys. Rev. Lett.* **89**, 102001 (2002); CLEO Collaboration, D.M. Asner *et al.*, *Phys. Rev. Lett.* **92**, 142001 (2004); BaBar Collaboration, B. Aubert *et al.*, *Phys. Rev. Lett.* **92**, 142002 (2004).

[17] CLEO Collaboration, G.S. Adams *et al.*, *Phys. Rev. Lett.* **94**, 012001 (2005).

[18] The following sample of potential model predictions for the E1 matrix elements (ordered according to the publication date) is displayed in Fig. 4: D. Pignon, C. A. Piketty, *Phys. Lett.* **B74**, 108 (1978); E. Eichten, K. Gottfried, T. Kinoshita, K.D. Lane, T.M. Yan, *Phys. Rev.* **D21**, 203 (1980); W. Buchmuller, G. Grunberg, S.-H. Tye *Phys. Rev. Lett.* **45**, 103 (1980), *Phys. Rev.* **D24**, 132 (1981); C. Quigg, J.L. Rosner, *Phys. Rev.* **D23**, 2625 (1981) (2 entries: $c\bar{c}$, $b\bar{b}$ potential, respectively); J. Baacke, Y. Igarashi, G. Kasperidus, *Z. Phys.* **C13**, 131 (1982); R. McClary, N. Byers, *Phys. Rev.* **D28**, 1692 (1983); P. Moxhay, J.L. Rosner, *Phys. Rev.* **D28**, 1132 (1983); H. Grotch, D.A. Owen, K.J. Sebastian, *Phys. Rev.* **D30**, 1924 (1984); S.N. Gupta, S.F. Radford, W.W. Repko, *Phys. Rev.* **D26**, 3305 (1982), *Phys. Rev.* **D30**, 2424 (1984); S.N. Gupta, S.F. Radford, W.W. Repko, *Phys. Rev.* **D34**, 201 (1986); M. Bander, D. Silverman, B. Klima, U. Maor, *Phys. Lett.* **B134**, 258 (1984), *Phys. Rev.* **D29**, 2038 (1984), *Phys. Rev.* **D36**, 3401 (1987); W. Kwong, J.L. Rosner, *Phys. Rev.* **D38**, 279 (1988); L.P. Fulcher, *Phys. Rev.* **D37**, 1259 (1988); S.N. Gupta, W.W. Repko, C.J. Suchyta III, *Phys. Rev.* **D39**, 974 (1989); L.P. Fulcher,

Phys. Rev. **D42**, 2337 (1990); A.K. Grant, J.L. Rosener, E. Rynes, *Phys. Rev.* **D47**, 1981 (1993); T.A. Lahde, *Nucl. Phys.* **A714**, 183 (2003).

[19] P. Moxhay, J.L. Rosner, *Phys. Rev.* **D28**, 1132 (1983); H. Grotch, D.A. Owen, K.J. Sebastian, *Phys. Rev.* **D30**, 1924 (1984); S.N. Gupta, S.F. Radford, W.W. Repko, *Phys. Rev.* **D30**, 2424 (1984); F. Daghighian, D. Silverman, *Phys. Rev.* **D36**, 3401 (1987); L.P. Fulcher, *Phys. Rev.* **D42**, 2337 (1990); D. Ebert, R. Faustov, V. Galkin, *Phys. Rev.* **D67**, 014027 (2003); T.A. Lähde, *Nucl. Phys.* **A714**, 183 (2003).

[20] The following sample of potential model predictions for the M1 matrix elements (ordered according to the publication date) is displayed in Fig. 6: V. Zambetakis, N.Byers, *Phys. Rev.* **D28**, 2908 (1983); H. Grotch, D.A. Owen, K.J. Sebastian, *Phys. Rev.* **D30**, 1924 (1984) (2 entries: scalar and vector confinement potential); S. Godfrey, N. Isgur, *Phys. Rev.* **D32**, 189 (1985) (2 entries: based on quoted transition moments and wave functions, respectively); X. Zhang, K.J. Sebastian, H. Grotch, *Phys. Rev.* **D44**, 1606 (1991) (2 entries: scalar-vector and pure scalar confinement potential); D. Ebert, R.N. Faustov, V.O. Galkin *Phys. Rev.* **D67**, 014027 (2003); T.A. Lahde, *Nucl. Phys.* **A714**, 183 (2003). Values of the M1 matrix elements in the $b\bar{b}$ system are displayed for the photon energies and b quark mass assumed in S. Godfrey, J.L. Rosner, *Phys. Rev.* **D64**, 074011 (2001), Erratum, *Phys. Rev.* **D65**, 039901 (2002).